

Baric Properties of InAs Quantum Dots

B. V. Novikov^a, G. G. Zegrya^b, R. M. Peleshchak^c, O. O. Dan'kiv^c, V. A. Gaisin^a,
V. G. Talalaev^{a, d, ^}, I. V. Shtrom^a, and G. E. Cirlin^{b, e, f}

^a Fock Institute of Physics, St. Petersburg State University, ul. Ulyanovskaya 1, St. Petersburg–Petrodvorets, 198504 Russia
[^]e-mail: talalaev@mpi-halle.mpg.de

^b Ioffe Physicotechnical Institute, Russian Academy of Sciences, Politekhnikeskaya ul. 26, St. Petersburg, 194021 Russia

^c Drogobych State Pedagogical University, ul. Ivana Franko 24, Drogobych, 82100 Ukraine

^d Max Planck Institute of Microstructure Physics, Weinberg 2, 06120 Halle, Germany

^e St. Petersburg Physics and Technology Centre for Research and Education, Russian Academy of Sciences,
ul. Khlopina 8 korp. 3, St. Petersburg, 195220 Russia

^f Institute of Analytical Instrument Making, Russian Academy of Sciences, Rizhskii pr. 26, St. Petersburg, 198103 Russia

Submitted November 20, 2007; accepted for publication December 5, 2007

Abstract—In the context of the deformation potential model, baric dependences of the energy structure of InAs quantum dots in a GaAs matrix are calculated. Under the assumption of the absence of interaction between the spherical quantum dots of identical sizes, the energy dependence of the baric coefficient of energy of the radiative transition in the quantum dot is determined. A similar dependence is also found experimentally in the photoluminescence spectra under uniform compression of the InAs/GaAs structures. Qualitative agreement between the theory and experiment as well as possible causes for their quantitative difference are discussed. It is concluded that such factors as the size dispersion, Coulomb interaction of charge carriers, and tunnel interaction of quantum dots contribute to this difference.

PACS numbers: 73.21.La, 78.55.Cr, 78.67.Hc, 81.40.Tv

DOI: 10.1134/S1063782608090133

1. INTRODUCTION

In recent years, successes in development of nanotechnology and physics of nanostructures had led to practical realization of some optoelectronic devices based on quantum dot (QD) arrays [1–3]. Being a quasi-zero-dimensional object, a QD has a discrete set of energy levels, sensitivity of which to stresses manifests itself even at the stage of QD nucleation during self-organization [4]. The kinetics of epitaxial growth and the stress distribution in the system QD–matrix affect the size, shape, and arrangement of QDs in the array [5, 6]. In this context, for an exact prediction of optical and transport properties of the QD array, it is necessary to construct an analytical model able to describe the following physical phenomena:

(i) dependence of the baric coefficient of the energy of the radiative transition between the ground states of the electron and hole in the QD (K_{QD}) on the size and shape of nanoislands;

(ii) the effect of strain-induced diffusion of adsorbed atoms on the shape and size of QDs;

(iii) interaction of the fields of local stresses with an electron subsystem QD–matrix and their effect on the profile of the quantization potential in the coherently stressed QD and in its vicinity; and

(iv) the electron-deformation mechanism of polarization of the QD.

In this paper, we report the results of studying the dependence of the baric coefficients of the energy of the radiative transition in the InAs QDs on their sizes for the InAs/GaAs heterosystem.

In most known cases, it is assumed that the deformation characteristics (the Young modulus and the Poisson coefficient) of nanoobjects coincide with corresponding bulk characteristics. However, the first studies of photoluminescence (PL) for the InAs/GaAs QD system [7–9] in the state of uniform compression showed that the baric coefficient for the InAs QDs differs from the baric coefficient of the energy of the radiative transition in bulk InAs ($K_{\text{InAs}} = 12$ meV/kbar). Moreover, it was shown in [8, 9] that the baric coefficient K_{QD} is not constant but depends on the energy of the radiative transition E_0 , i.e., on the QD size. This function was described well by the linear approximation. The dependence $K_{\text{QD}}(E_0)$ and its close-to-linear character were confirmed in [10, 11], involving compilation of the known experimental data. However, in some cases (molecules and multilayer QD arrays), we observed deviations of experimental points from the linear dependence [12]. This fact stimulated us to carry out the theoretical calculation of baric coefficients of the energy of the radiative transition in QDs of various sizes.

The known theoretical approaches for the stressed QD based on the use of perturbation theory [13] and the k_p method [14] were restricted to the obtaining of the dependence of the radiative transition energy E_0 on the pressure P and were used mainly for the description of the X- Γ intersection of the conduction band edges emerging at high pressures (42 kbar for the InAs QD). The first attempts to relate the baric coefficient K_{QD} to the QD sizes (with the energy of the PL peak) were attempted in [11] with the use of the Frogley model and in [15] based on the atomic model of the field of valence forces.

The purpose of this study is to describe the experimental dependence $K_{\text{QD}}(E_0)$ and its deviations for the QDs in the InAs/GaAs system in the context of the deformation-potential model.

2. MODEL OF THE InAs/GaAs HETEROSYSTEM WITH COHERENTLY STRESSED InAs QUANTUM DOTS

We consider the InAs/GaAs heterosystem with coherently stressed spherical InAs QDs. In order to reduce the problem with a large number of QDs to the problem with one QD, we use the following approximation. The energy of the pairwise elastic interaction between the QDs can be replaced by the energy of interaction of each QD with the averaged elastic strain field $\sigma_{\text{ef}}(N-1)$ of all other $(N-1)$ QDs.

Since the lattice constant of the InAs material is larger than that of the GaAs matrix, then, during heteroepitaxy in the limits of the pseudomorphic growth of InAs on GaAs, InAs is compression-strained while GaAs is tensile-strained. Therefore, the spherical QD can be represented as the elastic dilation microinclusion in the form of a sphere of radius R_0 (dash-dot line in Fig. 1a), which is incorporated into a spherical void of radius R_1 in the GaAs matrix (dashed line). The volume of the void is smaller than the volume of the microinclusion by ΔV . In order to insert such a spherical microinclusion, it is necessary to compress it in the radial directions and, contrarily, the GaAs matrix should be tensed in the limits of a sphere of radius R_2 . The solid line in Fig. 1a presents the result of simultaneous effect of these strains.

3. CALCULATION OF COMPONENTS OF THE STRAIN TENSOR IN THE SPHERICAL InAs QUANTUM DOT AND IN THE GaAs MATRIX

To determine the components of the strain tensor, it is necessary to find the explicit form of the displacements of atoms $u_r^{(1)}$ and $u_r^{(2)}$ in InAs and GaAs, respectively. For this purpose, let us write the equilibrium equation [16]

$$\nabla \operatorname{div} u = 0 \quad (1)$$

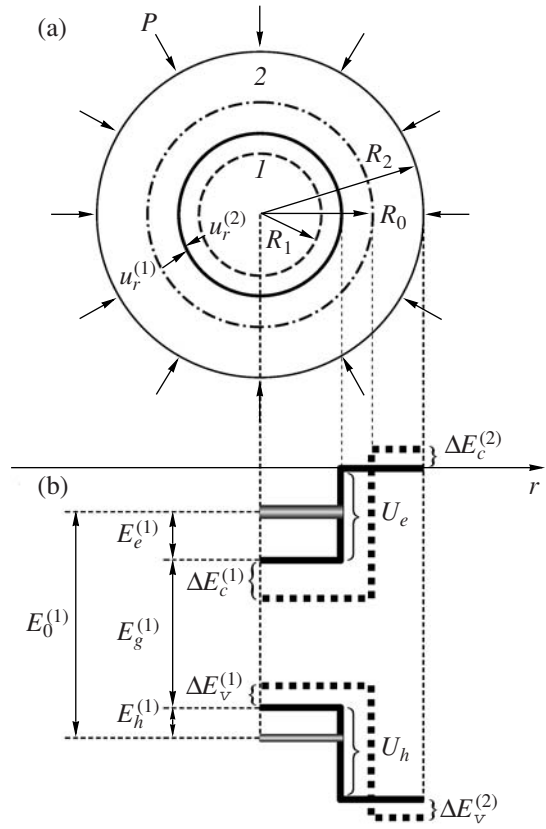


Fig. 1. (a) Model of spherical QD and (b) energy diagram of the structure (InAs QD)/GaAs matrix.

with the following boundary conditions for the spherical QD:

$$\begin{aligned} u_r^{(2)}|_{r=R_0} - u_r^{(1)}|_{r=R_0} &= fR_0, \\ |\sigma_{rr}^{(1)}|_{r=R_0} &= |\sigma_{rr}^{(2)}|_{r=R_0} + |P_L|_{r=R_0}, \end{aligned} \quad (2)$$

$$\sigma_{rr}^{(2)}|_{r=R_1} = -P - \sigma_{\text{ef}}(N-1), \quad P \gg \sigma_{\text{ef}}(N-1).$$

Here, R_0 is the QD radius, R_1 is the void radius in the GaAs matrix, and P is the hydrostatic pressure. The superscript (1) refers to InAs (QD), and the superscript (2) refers to GaAs (matrix). The Laplace pressure P_L is

$$P_L = \frac{2\alpha}{R_0 - |u_r^{(1)}|}, \quad (3)$$

where α is the surface energy of the InAs QD [17]. The difference of the volumes of the elastic dilation inclusion and the void in the GaAs matrix is $\Delta V = 4\pi R_0^3 f$. The parameter f is the sum of two terms,

$$f = f_1 + f_2.$$

The first term (f_1) is the mismatch parameter of strains caused by different coefficients of thermal expansion of

materials of the QD ($\alpha_T^{(1)} = 4.52 \times 10^{-6} \text{ K}^{-1}$) and matrix ($\alpha_T^{(2)} = 5.73 \times 10^{-6} \text{ K}^{-1}$):

$$f_1 = (\alpha_T^{(2)} - \alpha_T^{(1)})(T_K - T_0).$$

Here, T_K is the temperature of growth of the active region of the structure, and T_0 is the measurement temperature. The second term (f_2) is the lattice mismatch of the materials of the QD and the matrix ($a^{(1)}$ and $a^{(2)}$, respectively):

$$f_2 = \frac{a^{(1)} - a^{(2)}}{a^{(1)}} \approx 7\%.$$

The solution of Eq. (1) in the case of the spherical QD has the form [16, 18]

$$u_r^{(1)} = C_1 r + \frac{C_2}{r^2}, \quad 0 \leq r \leq R_0, \quad (4)$$

$$u_r^{(2)} = C_3 r + \frac{C_4}{r^2}, \quad R_1 \leq r \leq R_2. \quad (5)$$

Here, R_2 is the radius of the sphere of stress relaxation. Since at the point $r = 0$ the displacement should be finite, in solution (4) we assume that $C_2 = 0$. The field of displacements determines the following components of the strain tensor:

$$\varepsilon_{rr}^{(1)} = C_1, \quad (6)$$

$$\varepsilon_{rr}^{(2)} = C_3 - \frac{2C_4}{r^3}, \quad (7)$$

$$\varepsilon_{\theta\theta}^{(2)} = \varepsilon_{\theta\theta}^{(1)} = C_1, \quad (8)$$

$$\varepsilon_{\phi\phi}^{(2)} = \varepsilon_{\phi\phi}^{(2)} = C_3 + \frac{C_4}{r^3}. \quad (9)$$

Stresses in InAs and GaAs are correspondingly described by the relations

$$\sigma_{rr}^{(1)} = \frac{E_1}{(1 + \nu_1)(1 - 2\nu_1)} \quad (10)$$

$$\times [(1 + \nu_1)\varepsilon_{rr}^{(1)} + \nu_1(\varepsilon_{\phi\phi}^{(1)} + \varepsilon_{zz}^{(1)})],$$

$$\sigma_{rr}^{(2)} = \frac{E_2}{(1 + \nu_2)(1 - 2\nu_2)} \quad (11)$$

$$\times [(1 + \nu_2)\varepsilon_{rr}^{(2)} + \nu_2(\varepsilon_{\phi\phi}^{(2)} + \varepsilon_{zz}^{(2)})].$$

Here, ν_1 and ν_2 are the Poisson coefficients and E_1 and E_2 are the Young moduli of materials of the QD and surrounding matrix, respectively. They are expressed in the standard way in terms of the elastic constants of these materials. The coefficients C_1 , C_3 , and C_4 are determined from the solution of set of equations (2) taking into account (4)–(11).

The components of the strain tensor depend on the QD radius R_0 , QD shape, and hydrostatic pressure P and determine the energy shifts of the edges of allowed bands (conduction and valence band, respectively) caused by the elastic strain (Fig. 1b):

$$\Delta E_c^{(i)}(\varepsilon^{(i)}) = a_c^{(i)} \varepsilon^{(i)}, \quad \Delta E_v^{(i)}(\varepsilon^{(i)}) = a_v^{(i)} \varepsilon^{(i)}, \quad (12)$$

Here, $\varepsilon^{(i)} = \text{Sp} \hat{\varepsilon}^{(i)}$, $a_c^{(i)}$, and $a_v^{(i)}$ are the constants of the hydrostatic deformation potential of the conduction and valence bands.

4. CALCULATION OF BARIC COEFFICIENTS OF InAs QUANTUM DOTS IN THE InAs/GaAs HETEROSYSTEM. SIZE DEPENDENCE

Figure 1b shows the dependence of the potential energy of the electron and hole on the radius r in the InAs/GaAs heterosystem with the InAs QDs disregarding (dotted line) and taking into account (solid line) the effect of the uniform strain caused both by the lattice mismatch of the material of the QD and matrix and different thermal expansion coefficients and by the external hydrostatic pressure P . The energy levels of the electron (E_e) and hole (E_h) in the ground state are arranged in potential wells U_e and U_h , respectively:

$$U_e = \begin{cases} -(|\Delta V_e(0)| - |a_c^{(1)} \varepsilon^{(1)}| - |a_c^{(2)} \varepsilon^{(2)}|), & 0 \leq r \leq R_0, \\ 0, & R_0 \leq r \leq R_1; \end{cases} \quad (13)$$

$$U_h = \begin{cases} -(|\Delta V_h(0)| - |a_v^{(1)} \varepsilon^{(1)}| - |a_v^{(2)} \varepsilon^{(2)}|), & 0 \leq r \leq R_0, \\ 0, & R_0 \leq r \leq R_1. \end{cases} \quad (14)$$

Here, $\Delta V_e(0)$ and $\Delta V_h(0)$ are the depths of potential wells for the electron and hole in the InAs QD in the strain-free InAs/GaAs heterostructure.

The energy of the recombination transition between the ground states of the electron and hole with their Coulomb interaction disregarded is

$$E_0^{(1)} = E_e^{(1)} + E_h^{(1)} + E_g^{(1)}, \quad (15)$$

Here, $E_g^{(1)}$ is the band gap in the InAs QD.

The baric coefficient K_{QD} for the InAs QD in the InAs/GaAs heterosystem is determined by three components:

$$K_{\text{QD}} = \frac{\partial E^{(1)}}{\partial P} = \frac{\partial E_e^{(1)}}{\partial P} + \frac{\partial E_h^{(1)}}{\partial P} + \frac{\partial E_g^{(1)}}{\partial P} \quad (16)$$

$$= \frac{\partial \varepsilon^{(1)}}{\partial P} \frac{1}{\partial \varepsilon^{(1)} / \partial R_0} \left[\frac{\partial E_e^{(1)}}{\partial R_0} + \frac{\partial E_h^{(1)}}{\partial R_0} + \frac{\partial E_g^{(1)}}{\partial R_0} \right].$$

Here, $\partial E_c^{(1)}/\partial P$ is the component of the baric coefficient caused by the shift of the electron level under the effect of the hydrostatic pressure, $\partial E_h^{(1)}/\partial P$ is the component of the baric coefficient caused by the shift of the hole level under the effect of the hydrostatic pressure, and $\partial E_g^{(1)}/\partial P$ is the baric coefficient of the band gap.

To determine the baric coefficient K_{QD} (16), it is necessary to calculate the energy spectrum of the electron and hole in the InAs/GaAs heterosystem with the InAs QD. Since we carry out the calculation in the effective-mass approximation, we require the fulfillment of physical conditions under which the geometric sizes of the QD and spatial region between two neighboring QDs considerably exceed the lattice constants of InAs (a_d) and GaAs (a_m), i.e., the radius of the spherical QD $R_0 \gg a_d, a_m$. For the calculation, it is necessary to solve the Schrödinger equation

$$H_{e,h}\Psi_{e,h}(\mathbf{r}) = E_{e,h}\Psi_{e,h}(\mathbf{r}) \quad (17)$$

with the Hamiltonian

$$H_{e,h} = -\frac{\hbar^2}{2} \nabla \frac{1}{m_{e,h}^*} \nabla + U_{e,h}(\mathbf{r}, R_0, P). \quad (18)$$

We assume that the effective masses of the electron $m_{1e,2e}^*$ (hole $m_{1h,2h}^*$) in the QD and in the surrounding matrix are known and equal to bulk values.

The solution of the Schrödinger equation (17) in the spherical system of coordinates has the form

$$\Psi_{nlm}(r, \theta, \varphi) = R_{nl}(r)\Psi_{lm}(\theta, \varphi). \quad (19)$$

Here, $Y_{lm}(\theta, \varphi)$ are the spherical Legendre functions [19]. The radial functions $R_{nl}(r)$ are expressed in terms of the spherical Bessel functions:

$$R_{1nl}(r) = A j_l(k_{e,h}r) + B n_l(k_{e,h}r), \quad 0 \leq r \leq R_0, \quad (20)$$

$$R_{2nl}(r) = C h_l^{(1)}(i\chi_{e,h}r) + D h_l^{(2)}(i\chi_{e,h}r), \quad (21)$$

$$R_0 \leq r \leq R_1,$$

where

$$k_{e,h}^2 = \frac{2m_{1e,1h}^*}{\hbar^2} (|U_{e,h}| - |E_{nl}^{e,h}|), \quad (22)$$

$$\chi_{e,h}^2 = \frac{2m_{2e,2h}^*}{\hbar^2} |E_{nl}^{e,h}|, \quad (23)$$

while the potential energies of the electron and hole $U_{e,h}$ are determined by formulas (13) and (14). The continuity conditions for the wave functions and density of the flow of probability at the QD–matrix interface,

$$\begin{cases} R_1(r)|_{r=R_0} = R_2(r)|_{r=R_0}, \\ \frac{1}{m_{1e,1h}^*} \frac{dR_1(r)}{dr} \Big|_{r=R_0} = \frac{1}{m_{2e,2h}^*} \frac{dR_2(r)}{dr} \Big|_{r=R_0}, \end{cases} \quad (24)$$

along with the regularity condition of the functions $R_{nl}(r)$ at $r \rightarrow 0$ and $r \rightarrow R_1$ and with normalization determine the energy spectrum E_{nl} and wave functions of the electron and hole in the InAs/GaAs heterosystem with the InAs QD.

Therefore, the energies of the ground state of the electron and hole in the QD are determined from the following transcendental equation:

$$\begin{aligned} & k_{e,h} \tan\left(k_{e,h}R_0 - n\frac{\pi}{2}\right) \\ &= \chi_{e,h} \frac{m_{1e,1h}^*}{m_{2e,2h}^*} \frac{1 + \exp[2\chi_{e,h}(R_0 - R_1)]}{1 - \exp[2\chi_{e,h}(R_0 - R_1)]}, \end{aligned} \quad (25)$$

$$n = 1, 3, 5, \dots$$

Based on Eq. (25) and using (16), we can calculate the baric coefficients K_{QD} depending on the QD sizes taking into account that

$$\frac{\partial E_0}{\partial R_0} = -\frac{\partial f / \partial R_0}{\partial f / \partial E_c}, \quad \frac{\partial E_h}{\partial R_0} = -\frac{\partial \varphi / \partial R_0}{\partial \varphi / \partial E_h}, \quad (26)$$

where

$$\begin{aligned} f &= k_e \tan\left(k_e R_0 - n\frac{\pi}{2}\right) \\ &= \frac{\chi_e(m_{1e}^*/m_{2e}^*) [1 + e^{2\chi_e(R_0 - R_1)}]}{1 - e^{2\chi_e(R_0 - R_1)}}, \\ f &= k_h \tan\left(k_h R_0 - n\frac{\pi}{2}\right) \\ &= \frac{\chi_h(m_{1h}^*/m_{2h}^*) [1 + e^{2\chi_h(R_0 - R_1)}]}{1 - e^{2\chi_h(R_0 - R_1)}}. \end{aligned}$$

5. NUMERICAL CALCULATIONS AND DISCUSSION

Further, we present the results of theoretical studies of the dependence of the baric coefficient of the InAs QD (K_{QD}) on the energy of the recombination transition and on the QD radius (R_0), as well as the dependence of the shift of the transition energy (ΔE_0) on the hydrostatic pressure for various values of E_0 in the context of the deformation potential model. The calculations were performed for the following parameters (see [17, 20, 21]): $a^{(1)} = 6.08 \text{ \AA}$, $a^{(2)} = 5.65 \text{ \AA}$; $C_{11}^{(1)} = 0.833 \text{ Mbar}$, $C_{12}^{(1)} = 0.433 \text{ Mbar}$, $C_{11}^{(2)} = 1.223 \text{ Mbar}$, $C_{12}^{(2)} =$

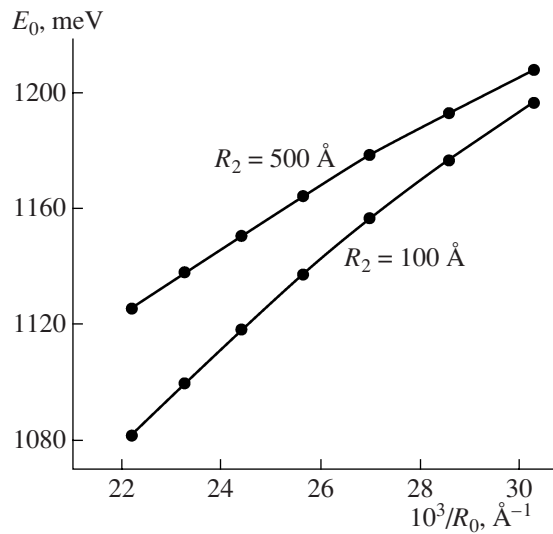


Fig. 2. Dependences of energy of the recombination transition E_0 on the inverse QD radius R_0 for values of the radius of the surrounding matrix $R_2 = 100$ and 500 Å.

0.571 Mbar; $\Delta V_c(0) = 0.6981$ eV, $\Delta V_v(0) = 0.3759$ eV; $a_c^{(1)} = -5.08$ eV, $a_c^{(2)} = -7.17$ eV, $a_v^{(1)} = 1$ eV; $a_v^{(2)} = 1.16$ eV; $E_g^{(1)} = 0.36$ eV, $E_g^{(2)} = 1.452$ eV; $m_{1e}^* = 0.057m_0$, $m_{2e}^* = 0.065m_0$, $m_{1h}^* = 0.41m_0$, $m_{2h}^* = 0.45m_0$; and $\alpha^{(1)} = 0.657$ N/m.

Figure 2 shows the dependence of the energy of the recombination transition on the inverse radius of the InAs QD in the InAs/GaAs heterosystem. It is evident that the transition energy E_0 increases monotonically as the QD radius R_0 decreases, and also increases with an increase in the radius R_2 of the matrix in which the QDs are formed. Specifically, a decrease in the QD radius from 45 to 35 Å leads to an increase in the transition energy by 93.7 meV at $R_2 = 100$ Å and by 66.8 meV at $R_2 = 500$ Å.

Using the dependences plotted in Fig. 2, we calculated the energy shift of the transition ΔE_0 for the InAs QD in the stressed InAs/GaAs heterostructure. The results of calculations graphically presented in Fig. 3 allow us to judge the increase in the considered shift with an increase in the hydrostatic pressure in the range of 0 – 15 kbar and its decrease with increasing QD size. It is known that the baric coefficient of the energy of the radiative transition of the bulk InAs crystal is $K_{\text{InAs}} = 12$ meV/kbar, while the baric coefficient of the InAs QD calculated in the context of the above model is $K_{\text{QD}} = 9.726$ meV/kbar at $R_0 = 42$ Å; i.e., the value of the baric coefficient for the InAs QD is smaller by 19% .

The dependences of the K_{QD} on the transition energy E_0 and on the QD size R_0 calculated using the formulas of the previous section are shown in Figs. 4a and 4b. The theoretical calculation in the context of the model suggested predicts a linear decrease in the baric coefficient

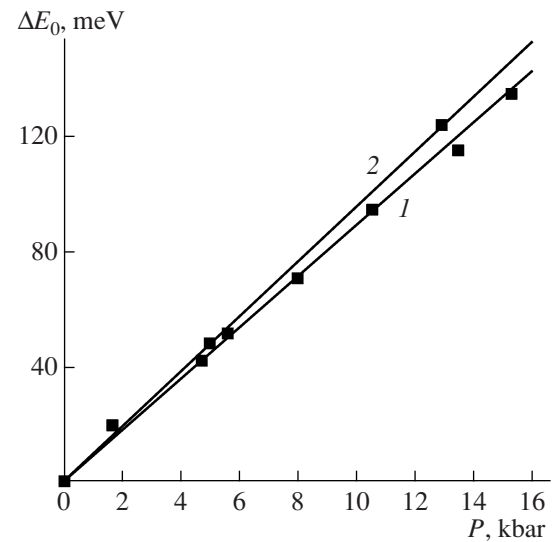


Fig. 3. Calculated dependences (solid lines) of the energy shift ΔE_0 of the InAs QD on the value of the hydrostatic pressure P for the values of the energy of the recombination transition (1) $E_0 = 1.13$ eV ($R_0 = 42$ Å) and (2) 1.15 eV ($R_0 = 39$ Å). Points correspond to the experimental shift of the PL band with the energy $E_0 = 1.23$ eV of the one-layer QD array at $T = 77$ K.

of the QD with increasing the energy of the recombination transition. According to this result, an increase in the QD size (i.e., narrowing of its optical gap) leads to a linear decrease in the baric coefficient

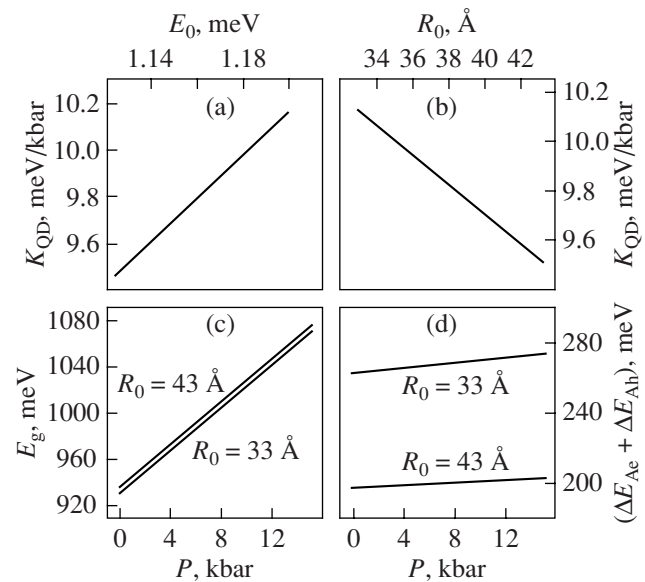


Fig. 4. Dependences of the baric coefficient in InAs QDs on the (a) energy of the recombination transition E_0 and the (b) QD size R_0 , (c) the component of the energy shift ΔE_0 caused by the dependence of the width of the optical band gap E_g of the QD on the hydrostatic pressure, and (d) the component of the energy shift ΔE_0 caused by the shift of the electron (ΔE_{Ae}) and hole (ΔE_{Ah}) level under the effect of the hydrostatic pressure.

K_{QD} . Specifically, the shift of the energy of the recombination transition from 1.15 to 1.13 eV corresponding to an increase in the QD size R_0 by 3 Å leads to a decrease in the baric coefficient by 0.1 meV/kbar.

Such a character of variation in the baric coefficient can be attributed to different characters of varying its components presented in Figs. 4c and 4d. As the QD size increases, a more rapid decrease in the component of the baric coefficient caused by the shift of the electron and hole levels under the effect of the hydrostatic pressure is observed (Fig. 4d) compared with the increase in the baric coefficient of the band gap (Fig. 4c).

6. EXPERIMENTAL RESULTS

We studied the PL spectra of the InAs QD arrays grown by molecular beam epitaxy on the GaAs substrates. The arrays differed by QD size (height) and the degree of their interaction. Such distinctions during the growth with the use of the same installation were provided by changes in technological parameters (growth mode, growth rate, temperature, and substrate misorientation) and by structural features of arrays (QD density in one layer, number of QD layers). The measurements were carried out at a hydrostatic pressure as high as 16 kbar (1.6 GPa) in a high-pressure chamber with leucosapphire mini-anvils. The chamber with a sample was placed into a cryostat, and the temperature in the cryostat was lowered to 77 K. The procedure is described in detail in [8]. Photoluminescence was excited by an argon laser with an emission power density of 0.2 kW/cm² and detected by a germanium photodiode or photomultiplier.

Figure 5 shows the original PL spectra of multilayer (stacked) QD arrays (QDSL) under the starting conditions (atmospheric pressure, 77 K) and at a maximum pressure of 16 kbar in the temperature range of 77–300 K. Such an array has a series of features previously studied by us in [22]. The array involves two size groups of QDs, namely, small stacked QDs on internal InAs layers (short-wavelength band C_0) and large associated QDs on the upper InAs layers (long-wavelength band A_0 corresponds to the transition between the ground states of the electron and the hole; the bands A_1 and A_2 correspond to transitions with the participation of excited states). Another feature of this array is the high degree of interaction between QDs in neighboring layers—the wave functions of QDs neighboring along the vertical overlap due to tunneling. In Fig. 5, blue shift of PL bands caused by the uniaxial compression, narrowing of the bands, and a difference in the blue shift for bands of different origin are easily distinguishable. For example, at a pressure of 16 kbar, the band C_0 of the “usual” QDs is shifted by almost 100 meV, while the band of associated QDs has a blue shift of A_0 of no more than 85 meV. The pressure dependence of the blue shift of the PL bands is represented in more detail in

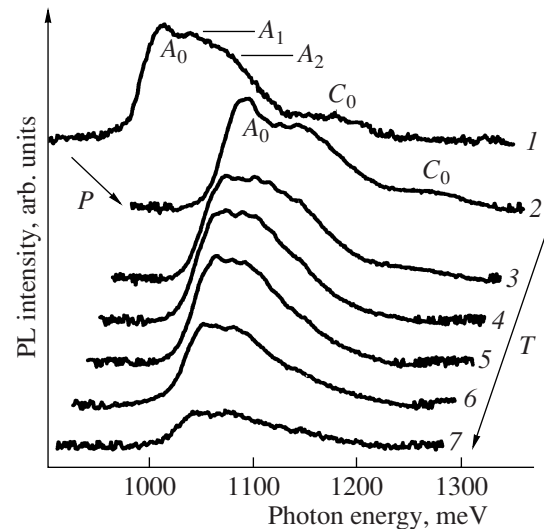


Fig. 5. Photoluminescence (PL) spectra of the ten-layer structure with the InAs QDs (QDSL): (1) without compression at 77 K, (2–7) under a pressure of 16 kbar at temperatures $T = 77, 100, 120, 160, 240,$ and 300 K, respectively.

Fig. 3. The baric coefficients calculated for the approximation by the linear dependence were 10.4 meV/kbar for the free exciton in GaAs, 6.1 meV/kbar for the usual QDs, and 5.2 meV/kbar for the associated QDs.

Similarly, we previously studied the compressed InAs QDs of various sizes in one-layer arrays (OQD) [8, 9, 23] and QD molecules in two-layer arrays (QDM) [24]. From the whole variety of QD OQD (about 15 arrays are studied), isolated QDs (IQD), that emerge on vicinal terraces at high degrees of their bundling with discontinuities of the layers on the steps should be especially noted. The interaction between such QDs is virtually absent [22, 25]. On the contrary, the interaction between the QDs forming the molecule is highly pronounced [26].

For all measured structures with the QDs of various sizes and types, we constructed the dependence of the energy of the radiative transition E_0 on the pressure P . As an example, Fig. 3 represents the experimental data of the dependence $E_0(P)$ for the PL band with $E_0 = 1.23$ eV of the one-layer QD array in comparison with the calculated dependences for $E_0 = 1.13$ and 1.15 eV. It is evident that the linear approximation of this dependence is a very good approximation. Based on this fact, from the slope of the straight line, we calculated the baric coefficients K_{QD} for all studied QDs. The values of K_{QD} were then brought into the dependence of K_{QD} on the energy E_0 represented in Fig. 6. For the QD states OQD, A_0 , and A_1 , the linear approximation was performed. For comparison of the experiment with the theory, we also present the straight line (solid line) in Fig. 6, which was theoretically calculated by us (see Fig. 4a). The comparison shows that only the data for the isolated IQD QDs exactly corresponds to the calculated straight line. The linear approximation for the

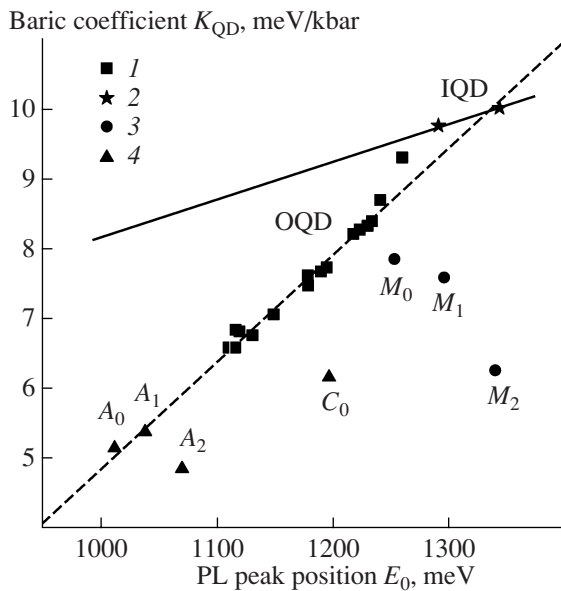


Fig. 6. Dependence of the baric coefficient K_{QD} on the energy of the radiative transition E_0 for various QD arrays: (1) OQD QDs in one-layer arrays; (2) isolated IQD QDs on vicinal substrates; (3) QD molecules QDM in two-layer arrays; and (4) stacks of the InAs/GaAs QDs (10 layers, spacer 8 nm), C_0 band corresponds to stacked QDs, and A_0 , A_1 , A_2 bands correspond to associated QDs. The dashed line is the linear approximation of the experimental data for the PL bands OQD, A_0 , and A_1 . The solid line is the theoretical calculation (see Fig. 4a).

OQD QDs is characterized by a slope of 15.5 bar^{-1} , while the theory predicts a slope of 5.5 bar^{-1} . The ground state of stacked QDs (C_0), second excited states of associated QDs (A_2), and all molecular terms ($M_{0,1,2}$) had the baric coefficients shifted to the region of smaller values relative to the data for OQD, A_0 , and A_1 in their approximation both by the straight line and by the parabola (Fig. 6).

Disagreement of the slopes of the calculated and experimental straight lines in the dependence $K_{\text{QD}}(E_0)$ can be explained by assumptions made while carrying out the calculations; specifically, identical size and spherical shape were prescribed to the nanoislands. In addition, in calculations, we disregarded the Coulomb interaction and the presence of the wetting layer, which is valid only for isolated QDs.

The size variance of QDs (by height) leads to the fact that the carrier distribution between the QDs in the array and, consequently, the contour of the PL line at this temperature are determined by the exchange processes between the QDs, i.e., by their interaction. Under the effect of uniaxial compression, the potential barriers and effective masses of carriers increase, and this process is more intense for smaller QDs having a larger baric coefficient. Due to this, the carriers are redistributed in favor of the increasingly growing part of deep potential wells. The external manifestations of this process are the retardation of the blue baric shift

because of the appearance of the “red” component (a decrease in K_{QD}) and narrowing of the PL band. We observed both effects experimentally (Figs. 5, 6). Similar narrowing of the PL band was also observed in [27].

We associate the deviation of the experimental dependence $K_{\text{QD}}(E_0)$ for QD stacks and molecules with a strong interaction of such states because of high transparency of the barrier (spacer) between the neighboring QDs. The emerging tunneling stimulates the effective carrier exchange. Due to this, the red component in the baric shift becomes more pronounced. The observed deviations are by essence a more pronounced manifestation of the effect considered above. This conclusion corresponds to the result obtained in [28], where the authors observed a decrease in the blue shift with an increase in pressure under a weak excitation in the stacked QDs with a very thin spacer (3 nm). In the context of the model suggested by us, this result corresponds to the extreme dominant increase in the red component in the spectral shift of the PL of the tunneling-coupled QD array.

7. CONCLUSIONS

Thus, the baric dependences of PL for the QD arrays with a number of layers of 1, 2, and 10 are studied experimentally. For the one-layer arrays, we confirmed the linear dependence of the baric coefficient on the energy of the ground state of the QD and thereby on the QD size, which was found previously for the first time. A theoretical model for the spherical noninteracting QDs under the conditions of uniaxial compression, which provides good agreement with the experiment for isolated QDs, is developed. Further development of the model is associated with allowing for the role of the wetting layer and the Coulomb interaction of the carriers in the QDs. The values of baric coefficients for the two-layer QD arrays (QD molecules) as well as for shallow-lying states in multilayer (stacked) QD arrays substantially deviate from the found linear dependence. The tunneling interaction of such states will be taken into account in the future in the course of improvement of the physical model of the QD array under conditions of hydrostatic compression.

ACKNOWLEDGMENTS

This study was supported by the Russian Foundation for Basic Research and by the Scientific Program of the Presidium of the Russian Academy of Sciences “Quantum Nanostructures.”

REFERENCES

1. V. P. Evtikhiev and O. V. Konstaninov, *Fiz. Tekh. Poluprovodn.* **36**, 79 (2002) [*Semiconductors* **36**, 74 (2002)].
2. N. N. Ledentsov, V. A. Shchukin, T. Kettler, et al., *J. Cryst. Growth* **301**, 914 (2007).

3. V. M. Ustinov, A. E. Zhukov, A. Y. Egorov, and N. A. Maleev, *Quantum Dot Lasers* (Oxford Univ. Press, Oxford, 2003).
4. N. N. Ledentsov, V. M. Ustinov, V. A. Shchukin, et al., *Fiz. Tekh. Poluprovodn.* **32**, 385 (1998) [*Semiconductors* **32**, 343 (1998)].
5. V. A. Shchukin and D. Bimberg, *Appl. Phys. A* **67**, 687 (1998).
6. V. G. Dubrovskii, Yu. G. Musikhin, G. É. Tsirlin, et al., *Fiz. Tekh. Poluprovodn.* **38**, 342 (2004) [*Semiconductors* **38**, 329 (2004)].
7. I. E. Itskevich, M. Henini, H. A. Carmona, et al., *Appl. Phys. Lett.* **70**, 505 (1997).
8. V. A. Gaĭsin, Din' shon Tkhak, B. S. Kulinkin, et al., *Vestn. St. Peterburg. Gos. Univ., Ser. 4, issue 4, No. 28*, 120 (2000).
9. V. A. Gaĭsin, Din' shon Tkhak, B. S. Kulinkin, et al., *Vestn. St. Peterburg. Gos. Univ., Ser. 4, issue 2, No. 12*, 115 (2001).
10. F. J. Manjon, A. R. Goni, K. Syassen, et al., *Phys. Status Solidi B* **235**, 496 (2003).
11. B. S. Ma, X. D. Wang, F. H. Su, et al., *J. Appl. Phys.* **95**, 933 (2004).
12. V. A. Gaisin, V. G. Talalaev, B. V. Novikov, et al., in *Proceedings of the 15th International Symposium "Nanostructures: Physics and Technology", Novosibirsk, Russia, 2007*, p. 212.
13. G. H. Li, A. R. Goni, K. Syassen, O. Brandt, and K. Ploog, *Phys. Rev. B* **50**, 18420 (1994).
14. S. I. Rybchenko, I. E. Itskevich, A. D. Andreev, et al., *Phys. Status Solidi B* **241**, 3257 (2004).
15. C. Kristukat, A. R. Goni, K. Potschke, et al., *Phys. Status Solidi B* **244**, 53 (2007).
16. C. Teodosiu, *Elastic Models of Crystal Defects* (Springer-Verlag, Berlin, 1982; Mir, Moscow, 1985).
17. E. Pehlke, N. Moll, and M. Scheffler, *Mater. Theory* **1**, 9607012 (1996).
18. L. D. Landau and E. M. Lifshitz, *Theory of Elasticity* (Mir, Moscow, 1965; Pergamon Press, Oxford, 1986).
19. S. Flugge, *Practical Quantum Mechanics* (Springer-Verlag, Berlin, 1971; Mir, Moscow, 1974).
20. A. Qteish and R. J. Needs, *Phys. Rev. B* **45**, 1317 (1992).
21. Chris G. Van de Walle, *Phys. Rev. B* **39**, 1871 (1989).
22. V. G. Talalaev, B. V. Novikov, M. A. Smirnov, et al., *Nanotechnology* **13**, 143 (2002).
23. V. A. Gaĭsin, Din' shon Tkhak, B. S. Kulinkin, et al., *Vestn. St. Petersburg. Gos. Univ., Ser. 4, issue. 1, No. 4*, 120 (2002).
24. V. A. Gaisin, B. V. Novikov, V. G. Talalaev, et al., in *Proceedings of the 13th International Symposium "Nanostructures: Physics and Technology", St. Petersburg, Russia, 2005*, p. 352.
25. V. G. Talalaev, B. V. Novikov, G. Gobsch, et al., *Phys. Status Solidi B* **224**, 101 (2001).
26. V. G. Talalaev, J. W. Tomm, N. D. Zakharov, et al., *Appl. Phys. Lett.* **85**, 284 (2004).
27. J. Phillips, P. Bhattacharya, and U. Venkateswaran, *Appl. Phys. Lett.* **74**, 1549 (1999).
28. S. I. Rybchenko, I. E. Itskevich, M. S. Skolnick, et al., *Appl. Phys. Lett.* **87**, 033104 (2005).

Translated by N. Korovin